Preprint of paper published as J. Phys.: Cond. Matter 15 (2003) pages 5649-5662

Modelling of compound semiconductors: Analytical bond-order potential for gallium, nitrogen and gallium nitride

J Nord†, K Albe‡, P Erhart‡and K H Nordlund†

† University of Helsinki, Accelerator Laboratory, P. O. Box 43, FIN-00014 University of Helsinki, Finland
‡ Technische Universität Darmstadt, Institut für Materialwissenschaft, Petersenstr. 23, D-64287 Darmstadt, Germany

E-mail: albe@hrzpub.tu-darmstadt.de

Abstract. An analytical bond-order potential for GaN is presented that describes a wide range of structural properties of GaN as well as bonding and structure of the pure constituents. For the systematic fit of the potential parameters reference data are taken from total energy calculations within the density functional theory if not available from experiments. Although long-range interactions are not explicitly included in the potential, the present model provides a good fit to different structural geometries including defects and high pressure phases of GaN.

Submitted to: *J. Phys.: Condens. Matter*

PACS numbers:

1. Introduction

Gallium nitride is a semiconducting compound material of high technological importance with a variety of applications in optoelectronics, high-power and high-temperature devices (Nakamura & Fasol 1997). An important requirement for the production of such devices is the modification of materials properties by controlled introduction of impurities into the material during growth or alternatively by ion implantation. On the other hand, despite of the impressive advances in the growth of GaN, even the best samples still contain high concentrations of as-yet-unidentified microscopic and mesoscopic defects. Therefore a fundamental understanding of growth mechanisms and processes like dopant implantation and defect formation is of great technological importance.

Atomic scale computer simulations, such as molecular–dynamics (MD) or kinetic Monte–Carlo (KMC) simulations, are nowadays a standard method to perform detailed investigations and allow to gain a deeper understanding of the relevant materials processes. For the success of any atomistic simulation, however, that can describe experimentally relevant time and lengths scales, computationally efficient and reliable interatomic potentials are a prerequisite condition. In the past much effort has been devoted to the development of such potentials for ionic oxides, covalent systems and metals. There are, however, only a few attempts to describe group–III nitrides by analytical interatomic potentials.

Gallium nitride is a semiconducting material with mixed covalent-ionic bonds. Therefore an analytical potential in principle has to include a proper description of both the chemical and electrostatic interactions. The latter is usually described by means of coulombic terms in the potential. Due to the long-range forces, however, the computational efficiency is significantly affected. On the other hand, many materials properties, such as amorphization behavior or stacking fault energies, can only be reproduced if the Coulomb interactions as well as the directional character of the covalent bonds are considered in the potential description.

In the past Zapol *et al.* (Zapol et al. 1997) have presented a two-body potential consisting of a long-range Coulombic part and a Buckingham form, where the shell-model approach was used for the nitrogen ions. Although the directional character of the covalent bonding usually requires angular terms, the authors argue that a sum of two body terms with partial charges can account for this. Their model reproduces the wurtzite, zinc-blende and rocksalt structures and was used to calculate defect and surface properties. Angularity was explicitly included in a potential proposed by Wang *et. al* (Wang et al. 2000), where the Coulomb term was combined with a Keating potential. In contrast, an emperical tight-binding formalism that explicitly neglects long-range forces has been derived by Boucher *et al.* (Boucher et al. 1999). Representing Ga and N with an sp^3–basis set they are able to reproduce some bulk and defect properties of GaN. Another short range potential based on the Stillinger–Weber formalism was proposed by Aïchoune *et al.* (Aïchoune et al. 2000) and used in a modified version for modelling dislocation core in GaN (Béré & Serra 2002).

All of these potentials give parameter sets for Ga–Ga and N–N mostly fitted from defect configurations. Structural properties of the pure constituents like the N_2 molecule or the α–Ga structure, however, are not considered in all previous studies and therefore simulations of surfaces (Northrup et al. 2000), defect clusters, growth or melting behavior are not possible.

In the present paper we devise a new analytical bond–order potential for GaN that is able to describe even the pure constituents. In doing so, we follow the same route as chosen in a preceeding paper on gallium arsenide (Albe et al. 2002), where the materials properties of the pure constituents were explicitly included in the fitting scheme. Although long-range interactions are formally neglected, the use of a short-ranged angular dependent potential for modelling the ionic-covalent interaction in GaN can partly be justified by the fact that Madelung energies for this compound are implicitly included in the input data set as taken from experiments or density functional theory (DFT) calculations.

The paper is organized as follows. First, we briefly review the basic algorithm of the potential. Then we give a short description of the fitting scheme and the parametrizations for nitrogen, gallium and GaN, seperately. Finally, we discuss the solubility of nitrogen ind liquid Ga as a first application of the current model.

2. Basic methodology and energy functional

In what follows we briefly report the analytical form of the potential which is discussed in detail in Ref. (Albe et al. 2002). The basic idea is to use a bond-order potential of the Tersoff-Brenner (Brenner 1989) form, where the total potential energy is written as a sum over individual bond energies:

$$E = \sum_{i>j} f_{ij}(r_{ij}) \left[V_{ij}^R(r_{ij}) - \underbrace{\frac{B_{ij} + B_{ji}}{2}}_{\overline{B_{ij}}} V_{ij}^A(r_{ij}) \right] . \tag{1}$$

The pairlike attractive and repulsive energies are given as Morse-like terms,

$$V^R(r) = \frac{D_o}{S-1} \exp\left(-\beta\sqrt{2S}(r-r_o)\right),$$
$$V^A(r) = \frac{SD_o}{S-1} \exp\left(-\beta\sqrt{2/S}(r-r_o)\right), \quad (2)$$

that depend on the dimer bond energy D_o, the dimer bond distance and the adjustable parameter S. The parameter β can be determined by the ground state oscillation frequency of the dimer. The interaction to the next neighbor sphere is restricted by a cutoff-function

$$f(r) = \begin{cases} 1, & r \le R-D, \\ \frac{1}{2} - \frac{1}{2}\sin\{\pi(r-R)/(2D)\}, & |R-r| \le D, \\ 0, & r \ge R+D \end{cases} \quad (3)$$

where D and R are adjustable quantities.

The bond-order parameter $\overline{B}_{ij}$ includes the angular dependencies, which are necessary to accurately model the deformation of covalent bonds:

$$B_{ij} = (1+\chi_{ij})^{-\frac{1}{2}},$$
$$\chi_{ij} = \sum_{k(\neq i,j)} f_{ik}(r_{ik}) g_{ik}(\theta_{ijk}) \exp[2\mu_{ik}(r_{ij}-r_{ik})]. \quad (4)$$

Here again the cutoff-function is included, while the indices monitor the type-dependence of the parameters, which is important for the description of compounds. The angular function $g(\theta)$ is given by:

$$g(\theta_{ijk}) = \gamma\left(1 + \frac{c^2}{d^2} - \frac{c^2}{[d^2 + (h+\cos\theta_{ijk})^2]}\right). \quad (5)$$

If r_b is the equilibrium bonding distance and E_b the energy per individual bond, a simple relation that sometimes is called Pauling-relation can be derived and is valid for any bonded structure independent of the specific choice for the bond-order term:

$$E_b = -D_o \exp\left(-\beta\sqrt{2S}(r_b - r_o)\right). \quad (6)$$

This equation is used to fit bond lengths and energies of structures with different atomic coordinations by adjusting parameters D_o, S, r_b and β.

3. Fitting procedure

The parameter sets for Ga-Ga, N-N, and Ga-N were adjusted independently. Those structures and properties, that are affected by the interplay of the different parameters were not included in the fitting procedure, but were analyzed later. The parameters in the pairlike terms were chosen in accordance to the dimer properties if possible, while the slope of the energy-bond relation was adjusted to the total energy data by varying S. Finally, elastic moduli and structural properties were fitted simultaneously using the Levenberg-Marquardt method (Press et al. 1992).

Table 1. Parameter sets for the three interaction types.

ij	Ga-Ga	N-N	Ga-N
γ	0.007874	0.76612	0.001632
S	1.11	1.4922	1.1122
$\beta(\text{Å}^{-1})$	1.08	2.05945	1.968
D_e(eV)	1.40	9.91	2.45
R_e (Å)	2.3235	1.11	1.921
c	1.918	0.178493	65.207
d	0.75	0.20172	2.821
$h = \cos(\theta_o)$	0.3013	0.045238	0.518
$2\mu(\text{Å}^{-1})$	1.846	0	0
R_{cut} (Å)	2.87	2.2	2.9
D (Å)	0.15	0.2	0.2

3.1. Gallium

The parametrization for the gallium interaction is the same as used before in the GaAs potential (Albe et al. 2002) (Table 1). In the context of the GaAs potential(Albe et al. 2002), however, the cutoff interval for Ga was taken as 2.8–3.1 Å. In GaN the next neighbor distance is shorter and therefore the cutoff-range for the Ga-Ga interaction was readjusted to 2.72-3.02 Å . This prevents that Ga atoms in the second neighbor shell are interacting with each other at low temperatures. This modification affects the thermal properties of the α-Ga structure as reported in Ref. (Albe et al. 2002), where the longest bond length is 2.7 Å with the current parameter set. We found that the melting point increases to 700(100) K with the modified range of the Ga-Ga interaction. In this context it should be noted that our cutoff range is similar to that chosen in the empirical TB potential of Boucher *et al.* (Boucher et al. 1999). In contrast to their work, however, we did not have problems to fit the elastic properties of the GaN compound structures using our first neighbor shell model.

3.2. Nitrogen

Diatomic nitrogen is characterized by strong triple covalent bonds and has among the highest binding energy of any molecule. At low temperatures and pressures it forms a molecular crystal with weak van–der–Waals interaction between molecules. It is the only group V element that does not polymerize to single-bonded systems as phosporous and arsenic (A7) do. A couple of years ago Mailhiot *et al.* (Mailhiot et al. 1992) presented a theoretical study based on DFT calculations. They investigated the stability of several crystalline structures and concluded that a cubic structure of nitrogen might form at pressures of about 50 GPa. In recent experiments Eremets *et al.* (Eremets et al. 2001) found evidence for a non-molecular structure of solid nitrogen forming at about 100 GPa which stays stable at ambient pressure for temperatures below 100 K. For fitting the Pauling relation shown in figure 1 we used Mailhots data on the high-symmetric metallic structures fcc, sc, bcc and diamond, but not the polymeric modifications.

It turned out that a reasonable description of all energies was only possible by choosing a ground state frequency of 1840 cm^{-1} that is somewhat lower than the theoretical prediction of 2291 cm^{-1}. The final parameter set provides a very good description of the reference bond lengths and energies. As can be seen from table 2 the theoretical bulk moduli as given by Mailhiot *et al.* (Mailhiot et al. 1992) are consistently higher than the values obtained with the analytical potential. This is a direct consequence of the choice for the parameter β or equivalently the lower ground state oscillation frequency ω of the diatomic molecule. At

Figure 1. Semi-logarithmic plot of the bond energy/bond length relation for different N-structures: Shown are results calculated with the analytical potential compared to LDA calculations of Mailhiot et al. (Mailhiot et al. 1992).

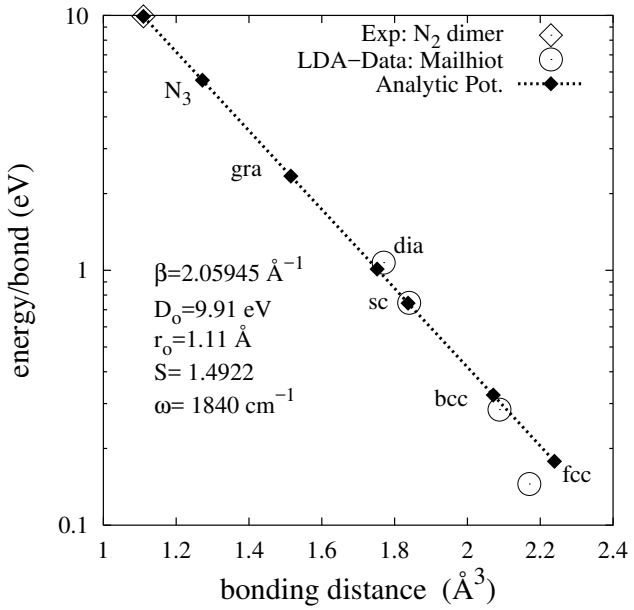

Table 2. Energy and structural parameters of different nitrogen phases.

N_2	LDA [(Mailhiot et al. 1992)]	Exper.	Anal. Pot.
r_o (Å)		1.11	1.11
D_o (eV)		9.91	9.91
ω_o (cm^{-1})		2291 (Huber & Herzberg 1979)	1840
lin.N_3			
r_o (Å)			1.272
E_{coh} (eV)			-3.712
graphite			
r_o (Å)			1.515
E_{coh} (eV)			-3.513
diamond			
a_o (Å^3)	4.10		4.044
E_{coh}. (eV)	-2.145		-2.022
B (GPa)	218.83		117.7
sc			
a_o (Å^3)	1.84		1.837
E_{coh}/f.u. (eV)	-2.235		-2.231
B (GPa)	228.21		175.7
bcc			
a_o (Å^3)	2.41		2.391
E_{coh} (eV)	-1.135		-1.297
B (GPa)	212.81		119.0
fcc			
a_o (Å^3)	3.08		3.167
E_{coh} (eV)	-0.895		-1.086
B (GPa)	167.68		101.3

this point the formalism is not flexible enough to reproduce the Pauling-relation using the reference value for ω.

With the current parameter set a number of quenching simulations were performed. From these we were not able to spot artificial spurious minima and the N_2 molecule always appeared as the thermodynamically stable ground structure.

3.3. Gallium Nitride

The increasing interest in GaN has not only stimulated a large number of experimental studies but also quantum-mechanical based calculations of bulk properties (Muñoz & Kune 1991, Kim et al. 1997, Shimada et al. 1998, Stampfl & van de Walle 1999, Serrano et al. 2000, Limpijumnong & Lambrecht 2001*a*, Limpijumnong & Lambrecht 2001*b*), defects (Neugebauer & Walle 1994, Boguslawski et al. 1995, Mattila et al. 1996, Mattila & Nieminen 1997, Gorczyca et al. 1999, Gorczyca et al. 1997, Northrup 2002) and surfaces (Northrup & Neugebauer 1996, Miotto et al. 1999, Northrup et al. 2000). The more ionic of the compound semiconductors exhibit a high-pressure phase transition from the tetrahedrally bonded structure to an octahedrally bonded structure, which has been investigated both experimentally (Ueno et al. 1994) and theoretically (Limpijumnong & Lambrecht 2001*a*) for GaN. In the present context we used results of density functional theory calculations on the structure and energy of different solid GaN phases of Serrano *et al.* (Serrano et al. 2000) as well as data of Muñoz and Kunc (Muñoz & Kune 1991).

The dimer properties of the diatomic molecule GaN have to our knowledge only been calculated by Kandalam *et al.*(Kandalam et al. 2000) using nonlocal density functional theory. They report a bond distance of 2.06 Å, which is well above the next neighbor distance in tetrahedrally bonded GaN, and therefore cannot be fitted with the present analytical formalism. We therefore decided to choose a dimer bonding distance of 1.921 Å , while keeping the bond energy at the theoretical value. Moreover, we found that the ground state

Figure 2. Semi-logarithmic plot of the bond energy/bond length relation for different GaN-structures: Shown are the results of the analytical potential and literature values of DFT-calculations (Muñoz & Kune 1991, Serrano et al. 2000, Kandalam et al. 2000)

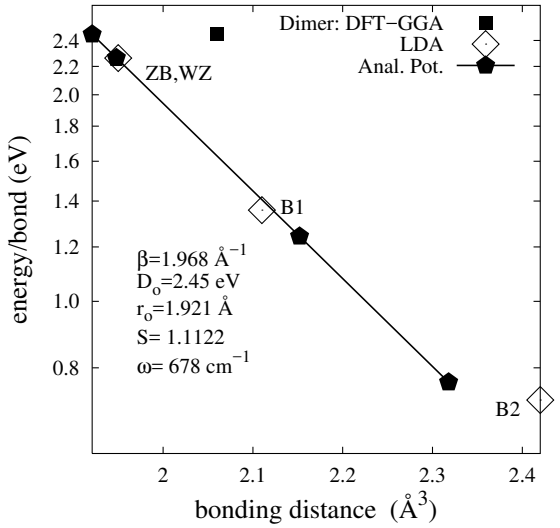

Table 3. Energy and structural parameters of different GaN-phases. Given are experimental values and theoretical results from DFT-calculations in comparison to the corresponding numbers as described with the analytical model.

GaN dimer	LCAO (Kandalam et al. 2000)	Exp. †	Anal. Pot.
r_o (Å)	2.06		1.921
D_o (eV)	2.45		2.45
ω_o (cm^{-1})	447		678
Zincblende GaN	LDA (Serrano et al. 2000)		
a_o (Å^3)	4.497	4.50	4.498
E_{coh}/f.u. (eV)	9.048		9.056
B (GPa)	196		205
B'	4.2		4.14
Wurtzite GaN			
a_o (Å^3)	3.180	3.190	3.180
c/a	1.632	1.627	1.633
r_o (Å^3)	1.948	1.956	1.948
u	0.376	0.377	0.375
E_{coh}/f.u. (eV)	9.058	9.058	9.056
E_{bond} (eV)	2.264	2.264	2.263
B (GPa)	196	188-245	205
B'	4.3	3.2-4.3	
T_{melt} (K)			
B1	LDA [(Muñoz & Kune 1991)]		
a_o (Å^3)	4.225		4.304
E_{coh}/f.u. (eV)	8.150		7.460
B (GPa)	240		233.0
B'	4.5		4.7
B2			
a_o (Å^3)	2.802		2.676
E_{coh}/f.u. (eV)	5.75		6.09
B (GPa)			230.8
B'			5.0

† Data reported in Ref. (Serrano et al. 2000)

oscillation frequency as determined by DFT-calculations (Kandalam et al. 2000) is too small to describe the bond stiffness, correctly. Therefore we adjusted the parameter β in such way that the bulk moduli of the solid GaN structures are well reproduced. After β and S were adjusted using the Pauling relation shown in figure 2, the remaining parameters were fitted by taking into account structures and energies of all high pressure phases listed in table 3 as well as elastic properties.

For fitting the bulk properties of GaN in wurtzite and high pressure structures the cohesive energies are required. Interestingly the values from literature are fairly diverse. If we take the cohesive energies of N_2 as 9.91 eV/molecule and 2.81 eV/atom for the cohesive energies of solid α-Ga, then the corresponding experimental values for the cohesive energy of w-GaN are 8.96 eV/f.u. (Harrison 1989), 9.4 eV/f.u. (Edgar 1994) and 11.4 eV/f.u. (Jones & Rose 1984). In the present context we took 9.058 eV/f.u. for the cohesive energy of w-GaN as reported in the work of Stampfl *et al.* (Stampfl & van de Walle 1999). This is close to the theoretical average of DFT calculations obtained in local and nonlocal approximation. All other energies listed in table 3 were taken relative to this number. With S=1.1122 the B2 (CsCl) as well as the B1 (NaCl) structure can be well reproduced. The calculated bulk modulus for the B1 phase is 233 GPa compared to 240 GPa from the LDFT-calculation (Serrano et al. 2000).

Table 4. Elastic constance for zinc-blende and wurtzite GaN. Lines label with a star (*) indicate elastic constants calculated with the transformation method of Martin(Martin 1972, n.d.).

ZB	Calc. †	Calc. †	Calc. †	Exp.†	Exp. †	Exp. †	CBP †	Anal. Pot
c_{11}	285	282	293				300	287
c_{12}	161	159	159				191	169
c_{44}	149	142	155				160	128
c^o_{44}	202		200					244
B	202	200	204				227	208
WZ								
c_{11}	350		367	390	365	377	386	347
$\star$	354	346	363				377	343
c_{12}	140		135	145	135	160	160	154
$\star$	150	148	147				183	159
c_{13}	104		103	106	114	114	141	123
$\star$	103	105	100				121	123
c_{33}	376	405	405	398	381	209	391	381
$\star$	401	389	410				440	379
c_{44}	101		95	105	109	81.4	115	81
$\star$	77	76	83				70	72
c_{66}	115		116	123	115	109	113	98
$\star$	101	99	108				97	92
B	197		202	210	204	173	227	208
$\star$	202	200	204				227	208

† LDA pseudopotential calculation (Shimada et al. 1998)
† FP-LMTO LDA calc. (Kim et al. 1997)
† LDA pseudopotential calculation (Wright 1997)
† Brillouin scattering (Polian et al. 1996)
† Brillouin scattering (Yamaguchi et al. 1997)
† Resonance Ultrasound (Schwarz et al. 1997)
† Coulomb-Buckingham potential (Zapol et al. 1997)

The elastic moduli of wurtzite GaN have been studied experimentally (Polian et al. 1996, Yamaguchi et al. 1997, Schwarz et al. 1997) and theoretically (Kim et al. 1996, Kim et al. 1997, Wright 1997, Shimada et al. 1998) by a number of groups. Their results are listed in table 4 and show significant deviations. This is most likely due to the fact that internal strain leads to atomic relaxations, which is treated differently by the relaxation procedures applied. Therefore we decided to fit the potential parameters to the elastic properties of zinc-blende GaN, where only the shear modulus c_{44} is affected by internal strain, and then to validate the results for *w*-GaN.

Since both structures are characterized by identical tetrahedral building blocks, the elastic tensor of the wurtzite structure ($c^w ij$) can be directly obtained from the moduli of the zinc-blende structure (c^z_{ij}), if structural differences of the third and fourth neighbor shells are negligible. Martin devised a transformation procedure (Martin 1972, n.d.) for wurtzite structures with an ideal c/a ratio and ideal displacement vector u, which can be summarized by

$$\begin{pmatrix} c^w_{11} \\ c^w_{12} \\ c^w_{13} \\ c^w_{33} \\ c^w_{44} \\ c^w_{66} \end{pmatrix} = \frac{1}{6} \begin{pmatrix} 3 & 3 & 6 \\ 1 & 5 & -2 \\ 2 & 4 & -4 \\ 2 & 4 & 8 \\ 2 & -2 & 2 \\ 1 & -1 & 4 \end{pmatrix} \begin{pmatrix} c^z_{11} \\ c^z_{12} \\ c^z_{44} \end{pmatrix} - \begin{pmatrix} \Delta^2/\overline{c^w_{44}} \\ -\Delta^2/\overline{c^w_{44}} \\ 0 \\ 0 \\ \Delta^2/\overline{c^w_{66}} \\ \Delta^2/\overline{c^w_{44}} \end{pmatrix}$$

with $\Delta = \frac{\sqrt{2}}{6}(c^z_{11} - c^z_{12} - 2c^z_{44})$ and $c^w_{66} = 1/2(c^w_{11} - c^w_{12})$. The unrelaxed moduli $\overline{c^w_{ij}}$ are obtained by applying the transformation matrix only without taking into account the second correction term. Since our short-ranged model potential cannot distinguish the different stacking sequences and predicts an ideal c/a ratio, it is appropriate for testing Martin's transformation method.

For fitting the elastic moduli, we have used the static elastic moduli for zinc-blende GaN as given by Shimamura *et al.*(Shimada et al. 1998). With the final parameter set all tensor components were calculated direcly by molecular statics allowing for full internal relaxations. The results compared to the transformation method and literature data are given in table 4. All elastic moduli are well reproduced within the uncertainty limits of the reference data. The relative differences of directly calculated values and those obtained by the transformation procedure are most significant for c_{44}. Since our model fullfills all formal criteria of the transformation method, these differences are due to relaxations of the 3. and 4. neighbor shells and some influence of the relaxation method. Please note, that the results reported by Zapol *et al.* (Zapol et al. 1997) for their Coulomb-Buckingham potential show a similarly good agreement with experiments and data calculated by DFT methods, although the bulk modulus is too high. The lacking angular dependency only seems to affect c^z_{12} and c^w_{13}.

4. Defect properties

Although there has been much progress in growing GaN during the last decade, there are many open questions related to native point defects and impurities. The sources of n-conductivity and yellow luminescence, for example, are still under discussion and the state of knowlegde on electronic properties of defects in GaN in general is still far from being complete, although there is a number of recent theoretical studies (Neugebauer & Walle 1994, Boguslawski et al. 1995, Mattila et al. 1996, Mattila & Nieminen 1997, Gorczyca et al. 1999, Gorczyca et al. 1997).

The formation energy of a defect in neutral charge state is given by

$$\Omega_D = E_{tot}(q) - n_{Ga}\mu_{Ga} - n_N\mu_N \tag{7}$$

where n_{Ga} and n_N are the number of gallium and nitrogen atoms and μ_{Ga} and μ_N the corresponding chemical potentials.

The chemical potentials of the pure constituents can vary depending on the chemical environment, but are limited by the chemical potentials of solid gallium μ^s_{Ga} and gaseous nitrogen $\mu^g_{N_2}$. Since the boundary condition $\mu_{Ga}+\mu_N = \mu^s_{GaN} = \mu^g_{N_2}+\mu^s_{Ga}+\Delta H_f$ applies, where μ^s_{GaN} is the chemical potential and ΔH_f the formation energy of *w*-GaN, respectively, the defect formation energy at zero temperature can be rewritten as follows (Qian et al. 1988):

$$\begin{aligned}&\Omega_D(\mu_{Ga},\mu_N) = \\ &\underbrace{E_D - \frac{1}{2}(n_{Ga}+n_N)\mu^s_{GaN} - \frac{1}{2}(n_{Ga}-n_N)(\mu^s_{Ga}-\mu^g_{N_2})}_{E'_D} \\ &- \frac{1}{2}(n_{Ga}-n_N)\Delta\mu \quad ,\end{aligned} \tag{8}$$

where $\Delta\mu$ is restricted to the range $-\Delta H_f < \Delta\mu < \Delta H_f$.

Fairly diverse results were reported in literature on the formation energies of interstitials, which strongly depend on the charge state, while the data for antisites and vacancies are widely consistent. A major caveat, however, in comparing our results with theoretical

values from literature is that different authors have been using fairly diverse values for the chemical potentials. In our calculation we have chosen $\mu^g_{N_2}$=9.91/2 eV, μ^s_{Ga}=2.81 eV and ΔH_f=1.29 eV, which are the formation energies of the corresponding structures as given by the present potential. Moreover, it should be noted that most total energy calculations are carried out at fixed volumes and therefore neglect the defect formation volumina.

Although the present analytic potential cannot account for charge effects, the basic requirement was to reproduce the hierarchy in formation energies of the different point defects, which are to a large extent determined by the significant difference in the atomic covalent radii of nitrogen and gallium atoms. Defects were investigated for a system that was thermally equilibrated at 600K and then slowly cooled down to 0 K at zero pressure. The defect formation energy then was determined from the potential energy E_D of the cell containing the defect.

The minimum energy position for interstitials was obtained by relaxing 100 cells with random interstitial position. All our defect simulations contained 64 atoms. Since strong internal relaxations may lead to finite size effects, simulations were repeated with a larger cell of 512 atoms.

The corresponding defect formation energies are given in table 5.

Table 5. Defect formation energies and volume changes for some defects in GaN. The values are for N-rich conditions unless otherwise stated. Energies are given in eV, formation volumes in Å^3.

defect	Ω_D 64 at.	Ω_D 512 at.	ΔV 512 at.	Ω_D †	Ω_D †	Ω_D †	Ω_D †
V_{Ga}	4.4	4.4	3.0	6.8		6.3	
V_N	1.5	1.4	-12	1.2		4.6	
V_{Ga} (Ga-rich)	5.7	5.7	3.0		8.5		8.1
V_N (Ga-rich)	0.2	0.1	-12		1.0		3.2
Ga_N	3.3	3.0	7.2	6.8		10.5	
N_{Ga}	5.9	5.2	7.7	5.2	5.7	5.8	
I_N	5.7	5.7	24	3.2			
I_{Ga}	5.5	5.5	22	4.1			

† LDA-DFT pseudopot. calc.,Ref. (Neugebauer & Walle 1994)
† LDA-DFT pseudopot. calc., calculated in ZB, Ref. (Mattila et al. 1996, Mattila & Nieminen 1997)
† DFT-LMTO calc., Ref. (Gorczyca et al. 1999)
† Car-Parinello, Ref. (Boguslawski et al. 1995)

Obviously, the potential is describing the nitrogen vacancy very well, which is the most important point defect in GaN. Even the other point defects are reproduced with good accuracy, taking into account the uncertainties of the reference data. Only the formation energy of the Ga antisite, which should be the energetically least favored defect, is significantly too small. Finite size effects are only significant for the antisite defects and the gallium vacancy, where atomic relaxations exceed the 64 atoms cell.

For the N-intersititial we find a minimum energy configuration in a split interstital state with N-N separation of 1.16 Å. The *ab-initio* calculations predict a similar configuration, but with a somewhat greater N-N separation of about 1.25 Å(Neugebauer & Walle 1994, Boguslawski et al. 1995). The equilibrium position of the Ga interstitial has been found to be strongly charge dependent in *ab-initio* (Neugebauer & Walle 1994) calculations. Our model predicts a displacement in the same direction as the DFT, but the relaxation is smaller (for the neutral charge state). However, for higher charge states the difference decreases due to the reduced relaxation in the *ab-initio* model. In wurtzite GaN there are two high symmetry

interstitial positions, *T* and *O*. The *T* site is located in the middle of nonbonded Ga and N atoms with two nearest neighbors and six next nearest neighbors.

The Ga(O) interstitial has six nearest neighbors and moves about 0.4 Å from the ideal position during relaxation, which is in agreement with DFT calculations. Also, the energy difference between T and O sites is small, as in *ab-initio* calculations.The energy difference of the Ga(O) and Ga(T) sites is found to be very small in our model in agreement with DFT calculations(Neugebauer & Walle 1994).

Here, it should be noted again that none of the defect properties reported here has been used for fitting the potential parameters, but are just the result of the potential formalism.

5. Melting point

The melting point of GaN is not known due to experimental difficulties related to the very high temperature and N_2 pressure necessary for melting. Experiments in a high pressure anvil cell showed that GaN does not melt at temperatures as high as 2573 K at 68 kbar (Edgar 1994).

For testing the melting behavior we used two kinds of simulations. One consisted of heating up crystalline cells until they melt, and subsequently cooling them slowly (over 100 ps - 10 ns) to 0 K, checking that the final structure is higher in potential energy than the desired ground state. Although this method is good for finding structures with energy minima far below the ground state, it is not good enough to spot minima lying just slightly lower ($\sim$ 0.1 eV) in energy than the desired state. To test the potential against such local minima, we used simulations of a liquid and solid in equilibrium (the same simulations were also used to determine the melting point, see below). If other energy minima are present, a phase transition to the lower minimum is likely to be initiated at the liquid-solid interface over long time scales.

The cutoff values of the potential were not systematically optimized in the fit of the potential to the different phases. Hence we could somewhat modify them to obtain a better fit to the melting point. Possible cutoff values were limited from below by the nearest neighbour distance of the fitted structures of materials. The second nearest neighbour defined an upper limit. The final cutoff was then chosen by testing several values between these limits for melting properties.

The melting properties of the potential model were tested by simulating a 5000 atom system at several temperatures and pressures. The simulation box, which initially consisted of liquid and crystalline phases, was equilibrated near the predicted melting point. Berendsen pressure control (Berendsen et al. 1984) to zero pressure was used in the melting simulations, independently in the x, y and z dimensions.

The equilibrated system was simulated for 1 - 5 ns at several temperatures. Since crystallization was observed at 3000 K and 20 kbar, and the system melted completely at 4000 K, we conclude that the melting point at this pressure is 3500$\pm$500 K. This is in a reasonable agreement with the theoretical estimate of the melting point of about 2791 K at 45 kbar (Vechten 1973).

6. Solubility

Additionaly, we employed the potential to study the solubility of atomic N in liquid Ga at temperatures and pressures typical for the direct high-pressure synthesis of GaN (Boćkowski 1999) using molecular dynamics (MD) and Monte-Carlo (MC) simulations. Initially, the simulation cell contained randomly phases of Ga and N_2 separated by a sharp interface. The system consisted of 1500 atoms and roughly twice as many Ga atoms as N

atoms. The sample was quenched in a MD simulation to 0 K and 0 kbar. This configuration was used for the MD as well as the MC runs. For the MD simulations the equations of motion were integrated for up to 4 ns at temperatures between 2000, and 3200 K and pressures between 20, and 200 kbar.

We used *NPT*-Monte Carlo to sample the configuration and volume space. The MC simulations essentially gave values within the errorbars of the MD results.

Figure 3. Solubility of N in liquid Ga as a function of temperature at a pressure of 200 kbar.

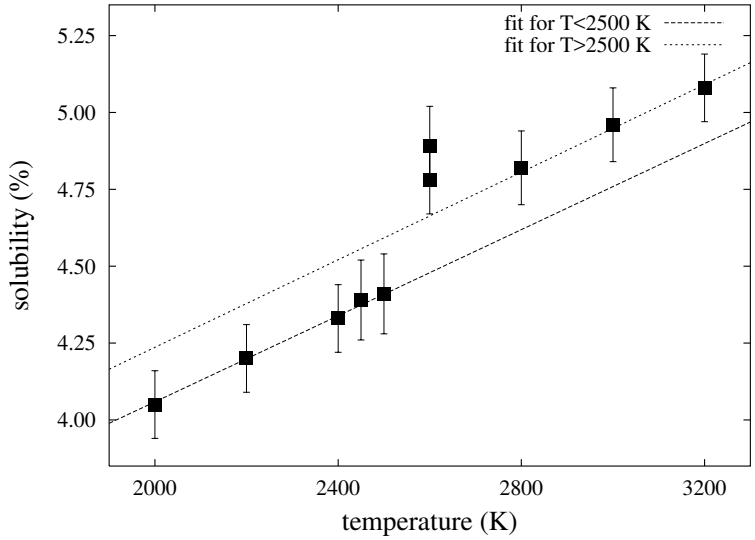

Figure 4. Solubility of N in liquid Ga as a function of pressure for temperatures between 2800 and 3200 K.

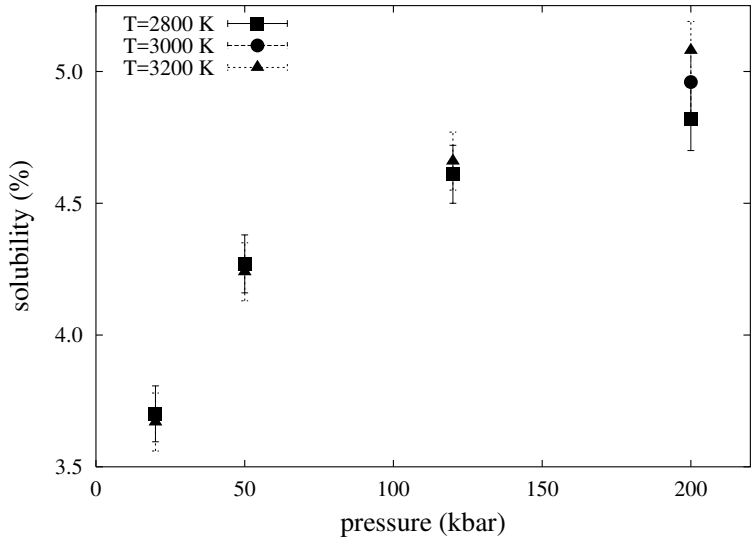

In order to distinguish atomic nitrogen and N_2 dimers a simple energy criterion was

applied. The potential energy of a dimer is known to be -4.9 eV. We determined that a cut-off energy of -4.1 eV allows a simple distinction of atomic nitrogen ($E_{pot} > -4.1\,eV$) and molecular nitrogen ($E_{pot} < -4.1\,eV$).

The nitrogen concentration in the Ga melt was plotted as a function of time to ensure that a steady-state had been reached. The solubility was calculated as the average over the equilibrated datapoints. Figure 3 shows the temperature dependence of the solubility of N in liquid Ga at a pressure of 200 kbar. At this pressure a clear trend of the solubility to increase with temperature can be observed. However, at lower pressures the solubility is found to be essentially unaffected by a raise in temperature. On the other hand, there is a pronounced pressure dependence for all temperatures tested here as illustrated in figure 4.

7. Conclusions

We have presented a new analytical potential for modelling Ga, As and GaN using a short-ranged bond-order algorithm. The potential describes with good accuray different dimer properties and several solid structures of the pure elements and the compound including metastable configurations. Important point defect properties, like the nitrogen vacancies, are in line with theoretial results from DFT-calculations. Moreover, the potential gives a reasonable description of melting behavior and solubility of nitrogen. This is to our knowledge the only classical potential that describes structure and bonding of Ga, N and GaN within one analytical form and therefore allows atomistic computer simulations of a wide range of materials problems related to GaN. Most importantly, this study shows that a number of relevant materials properties of GaN without including long-range forces. The energy difference of wurtzite and zinc blende, however, cannot be described with the current approach. Wherever these subtleties do not affect the materials process one wants to simulate, this new GaN potential should be an appropriate model for atomistic computer simulations of GaN.

8. Acknowledgements

The research was supported by the Academy of Finland under projects No. 46788 and 51585. Grants of computer time from the Center for Scientific Computing in Espoo, Finland are gratefully acknowledged.

This joined study was made possible by the support of the finish academy of science and the german foreign exchange server (DAAD) through a bilateral travel program.

References

n.d. The Q vector is misstyped in Ref.s (Martin 1972, Kim et al. 1996). It should read as: $Q = \sqrt{2}/6[1\,-\,1\,-\,2]$.
Aïchoune N, Potin V, Ruteran P, Hairie A, Nouet G & Paumier E 2000 *Comp. Mat. Sci.* **17**, 380–383.
Albe K, Nordlund K, Nord J & Kuronen A 2002 *Phys. Rev. B* **66**, 035205.
Béré A & Serra A 2002 *Phys. Rev. B* **65**, 205323.
Berendsen H, Postma J, van Gunsteren W, DiNola A & Haak J 1984 *J. Chem. Phys.* **31**, 3684.
Boćkowski M 1999 *Physica B* **265**, 1–5.
Boguslawski P, Briggs E L & Bernholc J 1995 *Phys. Rev. B* **51**(23), 17255.
Boucher D E, DeLeo G G & Fowler W B 1999 *Phys. Rev. B* **59**(15), 10064 – 10070.
Brenner D 1989 *Phys. Rev. Lett.* **63**(9), 1022.
Edgar J 1994 *Properties of group III-nitrides* Inspec London.
Eremets M I, Hemley R, Mao H & Gregoryanz E 2001 *Nature* **411**, 170.
Gorczyca I, Svane A & Christensen N 1997 *Solid State Comm.* **101**(10), 747–752.
Gorczyca I, Svane A & Christensen N E 1999 *Phys. Rev. B* **60**(11), 8147.

Harrison W 1989 *Electronic structure and the properties of solids* Dover Publications.
Huber K & Herzberg G 1979 *Constants of diatomic molecule* Van Nostrand Reinhold New York.
Jones R & Rose K 1984 *CALPHAD* **8**, 343.
Kandalam A, Pandey R, Blanco M, Costales A, Recio J & Newsam J 2000 *J. Phys. Chem. B* **104**, 4361–4367.
Kim K, Lambrecht W & Segall B 1996 *Phys. Rev. B* **53**(24), 16310–16326.
Kim K, Lambrecht W & Segall B 1997 *Phys. Rev. B* **56**(11), 7018–7019.
Limpijumnong S & Lambrecht W 2001*a* *Phys. Rev. Lett.* **86**(1), 91.
Limpijumnong S & Lambrecht W 2001*b* *Phys. Rev. B* **63**(1), 104103.
Mailhiot C, Yang L & McMahan A 1992 *Phys. Rev. B* **46**, 14419.
Martin R 1972 *Phys. Rev. B* **6**(12), 4546.
Mattila T & Nieminen R M 1997 *Phys. Rev. B* **55**(15), 9571.
Mattila T, Seitsonen A & Nieminen R M 1996 *Phys. Rev. B* **54**(3), 1474.
Miotto R, Srivastava G & Ferraz A 1999 *Phys. Rev. B* **59**(4), 3008.
Muñoz A & Kune K 1991 *Phys. Rev. B* **44**(18), 10372.
Nakamura S & Fasol G, eds 1997 *The blue laser diode - GaN-base light emitters and lsers* Springer Berlin.
Neugebauer J & Walle C G V D 1994 *Phys. Rev. B* **50**(11), 8067.
Northrup J 2002 *Phys. Rev. B* **66**, 045204.
Northrup J & Neugebauer J 1996 *Phys. Rev. B* **53**(16), 10477.
Northrup J, Neugebauer J, Feenstra R & Smith A 2000 *Phys. Rev. B* **51**(15), 9932.
Polian A, Grimsditch M & Grzegory I 1996 *J. Appl. Phys.* **79**, 3343.
Press W, Teukolsky S, Vetterling W & Flannery B 1992 *Numerial Recipes in Fortran* Cambride University Press Cambridge.
Qian G X, Martin R & Chadi D 1988 *Phys. Rev. B* **38**(11), 7649.
Schwarz R, Khachaturyan K & Weber E 1997 *Appl. Phys. Lett.* **70**, 1122.
Serrano J, Rubio A, Hernández E, Muñoz A & Mujica A 2000 *Phys. Rev. B* **62**(24), 16612.
Shimada K, Sota T & Suzuki K 1998 *J. Appl. Phys.* **84**(9), 4951–4958.
Stampfl C & van de Walle C 1999 *Phys. Rev. B* **59**(9), 5521.
Ueno M, amd A. Onodera M Y, Shimomura O & Takemura K 1994 *AIP Conf Proc* **309**(1), 557–560.
Vechten J A V 1973 *Phys. Rev. B* **7**(4), 1479–1507.
Wang S Q, Wang Y M & Ye H Q 2000 *Appl. Phys. A* **70**(4), 475 – 480.
Wright A F 1997 *J. Appl. Phys.* **82**(6), 2833.
Yamaguchi M, Yagi T, Azuhata T, Sota T, Suzuki K, Chichibu S & Nakamura S 1997 *J. Phys.: Condens. Matter* **9**, 241.
Zapol P, Pandey R & Gale J 1997 *J. Phys.: Condens. Matter* **9**, 9517–9525.